J Mol Model (2015) 21: 6
DOI 10.1007/s00894-014-2548-2

ORIGINAL PAPER

Theoretical study of the dimerization of aqueous beryllium cations

Xiaoyan Jin · Hai Wu · Hong Wang · Zhengjie Huang · Hong Zhang

Received: 22 September 2014 / Accepted: 24 November 2014 / Published online: 22 January 2015

Abstract The dimerization of monomeric beryllium species was studied via density functional theory (DFT) calculations, and the influences of deprotonation and substitution with various halide anions on the polymerization were explored. The results indicate that the dimerization was accomplished by aggregation followed by a nucleophilic attack reaction, and the hydrolysis that provides the nucleophilic hydroxyl group is a prerequisite for polymerization. An activation energy of 49.7 kJ mol^{-1} and an aggregation energy of −52.2 kJ mol^{-1} were found for the formation of $Be_2(OH)(H_2O)_6^{3+}$, indicating a exothermic reaction. Deprotonation promotes aggregation and increases the energy barrier to activation. Replacing a bound water with an F^- anion makes aggregation more thermodynamically favorable, but it does not significantly change the energy barrier. It was concluded that the charge and electronegativity of the anion are crucial influences on the energy of the activation barrier, whereas the aggregation energy is influenced not only by the charge but also by the symmetry of the bridging structure in the aggregate.

Keywords Dimerization process · Aqueous beryllium species · Substituting anions · Nucleophilic attack · DFT

Introduction

Beryllium is of great importance due to its widespread use in industrial applications [1, 2]. However, the high toxicity of its ions and compounds has become a serious obstacle to investigating beryllium chemistry [3–6]. Since the toxicity of beryllium is strongly related to equilibria in aqueous solutions [1, 7], gaining insights into aqueous beryllium species leads to a deeper understanding of beryllium chemistry.

As it is the smallest metal ion, the beryllium cation (radius: 35 pm) possesses a high charge density in aqueous solution [4, 8], and it inevitably exhibits a relatively strong tendency to form a wide variety of aqueous monomeric and polymeric beryllium species via hydrolysis–polymerization reactions. Many experiments have shown that the four-coordinate $[Be(H_2O)_4]^{2+}$ is stable at pH<3 in aqueous solution [9–12]. As the pH rises, the production of a series of deprotonated species such as $[Be(OH)(H_2O)_3]^+$, $[Be(OH)_2(H_2O)_2]$, and $[Be(OH)_4]^{2-}$ though the hydrolysis of $[Be(H_2O)_4]^{2+}$ leads to precipitation followed by dissolution [4]. Meanwhile, monomeric berylliums tend to polymerize, leading to various beryllium polymers with bridging hydroxyl groups, including the dimer [13], trimer [9], tetramer [14], etc. This behavior is broadly similar to that observed for the neighboring element aluminum. However, progress in beryllium solution chemistry has considerably lagged behind progress in the chemistry of aqueous aluminum species due to the aforementioned toxicity of beryllium. Moreover, reports on beryllium chemistry have mostly focused on theoretical approaches rather than experimental techniques for the same reason [15–17]. In earlier theoretical studies, the geometries of monomeric and polymeric beryllium clusters were optimized at the appropriate computational level and the NMR shielding of ^9Be was obtained; all of these calculated parameters were found to agree with their corresponding experimental values [15, 18]. Considering that the conversion processes that produce these beryllium species are sensitive to pH, the hydrolysis constants of monomeric beryllium have been estimated theoretically in previous studies, and those computational results were found to be consistent with the corresponding experimental values [17, 19]. Such results indicate that appropriate theoretical methods for investigating aqueous beryllium species have now been established.

X. Jin (✉) · H. Wu · H. Wang · Z. Huang · H. Zhang
School of Chemistry and Materials Engineering, Fuyang Teachers College, Fuyang, Anhui 236041, China
e-mail: gold-2004@126.com

Compared with monomeric beryllium species, polymeric beryllium has only rarely been reported due to the experimental difficulties involved in capturing such polymers, as well as their toxicity. Among beryllium polymers, the dimeric species is the most important because it is the initial product of the polymerization of monomeric beryllium and it is a reactant in subsequent polymerization reactions. Obviously, the formation of the beryllium dimer is crucial to the overall polymerization process. In this work, the dimerization process was simulated via density functional theory, and the influences of deprotonation and substitution with various halide anions on the dimerization were explored at the molecular level.

Computational details

All calculations were carried out with the GAUSSIAN 03 software package [20]. First, the ground-state equilibrium geometries of the monomeric and dimeric beryllium species were optimized at the B3LYP/6–311+G(d,p) level of theory [21–23]. The transition states of the dimerization reactions were found using the QST procedure at the same level of theory. Subsequently, vibrational frequencies of the optimized structures were computed to confirm the true minima on potential energy surfaces or transition states. Intrinsic reaction coordinate (IRC) calculations were performed for the transition states to confirm the corresponding reactants and products [24, 25]. Atomic charges were obtained from natural population analysis (NPA). Single-point energies were computed by the polarizable continuum model (PCM) [26, 27] with a dielectric constant of 78.39 and united atom radii at the computational level of MP2/6–311+G(d,p) [28].

It is well known that solvation effects should be taken into account when determining appropriate models for aqueous species. There are commonly both explicit and implicit solvation effects. Previous studies suggest that the implicit solvation effect has no influence on the structures of aqueous beryllium species, but they lower the energy of the activation barrier in water exchange reactions [8, 29]. With respect to the explicit solvation effect, the number of solvent water molecules added and the orientations of the hydrogen bonds as well as the interactions between hydrogen bonds all increase the uncertainty in the computational results when the whole solvation sphere is considered [29]. It is reported that the participation of just one solvent molecule in the reaction can be used to represent the explicit solvation effect for an aqueous beryllium cluster [29, 30]. Therefore, in the present work, single-point energies were computed to estimate the implicit solvation effect, and the participation of one solvent molecule in the reaction was used to simulate the explicit solvation effect.

Results and discussion

The formation of $Be_2(OH)(H_2O)_6^{3+}$

The process of polymerizing two monomeric berylliums to form one dimer is shown in Fig. 1, and the corresponding structural parameters are listed in Table 1. It can be seen that, at the beginning of the reaction, the monohydroxy complex $Be(OH)(H_2O)_3^+$ formed by hydrolysis approaches the fully hydrated $Be(H_2O)_4^{2+}$, prompting the formation of an aggregate which is also the reactant (R). This aggregate is regarded as an important precursor to the formation of the bridging structure, as proposed in earlier studies on the polymerization processes of other metal ions [31–33]. In the aggregate, two of the bound water molecules in $Be(H_2O)_4^{2+}$ are hydrogen-bonded to the hydroxyl of $Be(OH)(H_2O)_3^+$. Subsequently, the beryllium center in $Be(H_2O)_4^{2+}$ is attacked by the nucleophilic hydroxyl in $Be(OH)(H_2O)_3^+$, leading to the formation of a transition state (TS). The hydrogen bonds gradually disappear. Note that the distance between the beryllium center in $Be(H_2O)_4^{2+}$ and the hydroxyl in $Be(OH)(H_2O)_3^+$ varies from 3.496 to 2.184 Å, and the tetrahedral $Be(H_2O)_4^{2+}$ is transformed into a five-coordinate trigonal bipyramidal geometry, where the equatorial plane is composed of the three water molecules originally bound in $Be(H_2O)_4^{2+}$ while the remaining bound water molecule is located axially. For the axial water molecule, the extremely elongated (relative to that in the original tetrahedron) Be–OH_2 bond is close to the axial Be–OH distance (Table 1), implying that the trigonal bipyramid is symmetric. In contrast, no appreciable changes in the Be–OH_2 distances were found for the three equatorial water molecules. Afterwards, the dimeric product (P) forms as the axial water molecule continues to move away from the central beryllium. In this product, the Be–OH_2 distance lengthens to 3.422 Å in the axial direction and the Be–OH distance

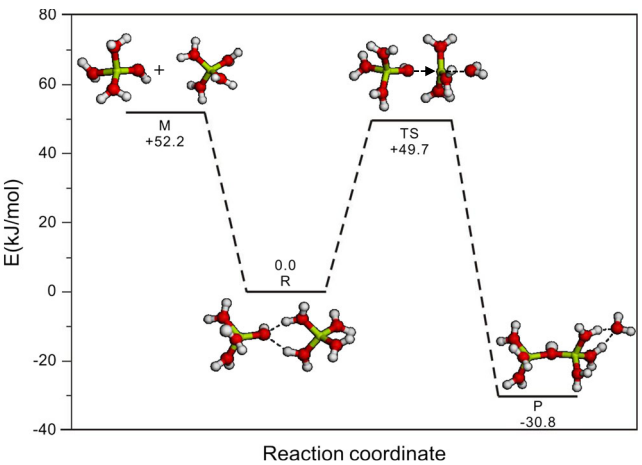

Fig. 1 Energy profile for the formation of $Be_2(OH)(H_2O)_6^{3+}$. *M* nonaggregated monomeric beryllium, *R* reactant, *TS* transition state, *P* product

Table 1 Bond lengths (Å) and bond angles (°) during the formation of $Be_2(OH)(H_2O)_6^{3+}$

	$Be(H_2O)_4^{2+}$			$Be(OH)(H_2O)_3^{+}$		Be–Be	∠Be–OH–Be
	Be–OH[a]	$Be–OH_2$	$Be–OH_2$(L)[b]	Be–OH	$Be–OH_2$		
R	3.496	1.640	1.659	1.577	1.698	4.958	
		1.649			1.696		
		1.656			1.686		
TS	2.184	1.643	2.028	1.575	1.700	3.642	
		1.647			1.708		
		1.664			1.692		
P	1.637	1.662	3.422	1.613	1.684	3.105	145.7°
		1.690			1.681		
		1.656			1.675		

[a] Distance between the nucleophilic hydroxyl and the attacked beryllium center

[b] Distance between the leaving water molecule and the attacked beryllium center

shortens to 1.637 Å, indicating that the axial water leaves the first coordination sphere, which is hydrogen-bonded to the two bound water molecules. Thus, the five-coordinate transition state is converted into a tetrahedral product with a single hydroxyl bridge connecting the two central beryllium atoms and a bond angle ∠Be–OH–Be of 145.7°.

During the course of polymerization, there is almost no change in the structure of $Be(OH)(H_2O)_3^{+}$ as compared with that of the fully hydrated $Be(H_2O)_4^{2+}$. As a matter of fact, the monohydroxy complex acts as the nucleophilic reagent that provides the attacking hydroxyl. From Table 1, we can see that the Be–OH distance increases when the terminal hydroxyl is transformed into a bridging hydroxyl. On the whole, the Be–OH_2 bond lengths in $Be(OH)(H_2O)_3^{+}$ are longer than those in $Be(H_2O)_4^{2+}$, which is thought to be due to the reduced positive charge on the metal atom in $Be(OH)(H_2O)_3^{+}$. Turning our attention to the energies, the aggregate is more stable than the two nonaggregated monomeric berylliums (M) by −52.2 kJ mol^{-1}, implying a strong tendency to aggregate. Meanwhile, an energy barrier of 49.7 kJ mol^{-1} was calculated for the nucleophilic attack reaction, and a reaction energy of −30.8 kJ mol^{-1} relative to the reactant indicates exothermic character. In addition, a gas-phase single-point energy computation was performed to estimate the implicit solvent effect. As shown in Table 2, the implicit solvent effect reduces the energy barrier by 50 %, in agreement with the conclusion drawn by Eldik et al. [29]. The reaction energy and aggregation energy both decrease greatly upon solvation.

Table 2 Influence of the implicit solvent effect on the energy parameters during the formation of $Be_2(OH)(H_2O)_6^{3+}$ (all values in kJ mol^{-1})

	Gas-phase reaction energy	Implicit solvent effect
M	281.2	52.2
R	0.0	0.0
TS	100.3	49.7
P	−30.8	−1.8

Influence of deprotonation on the dimerization process

As the polymerization is triggered by elevated pH, the dimerization reaction between two deprotonated beryllium species was studied in order to roughly estimate the influence of pH on the polymerization. As shown in Fig. 2, the two monohydroxy berylliums initially aggregate by forming two OH–OH_2 hydrogen bonds (i.e., an $H_3O_2^{-}$ bridge). The aggregation energy of 104.5 kJ mol^{-1} indicates a strong tendency to aggregate relative to the formation of $Be_2(OH)(H_2O)_6^{3+}$. This may be due to the fact that the reduced apparent charge on the cluster weakens the electrostatic repulsion between the beryllium species, thereby promoting aggregation. As a consequence, the Be–Be distance in the aggregate is shorter than that in the abovementioned $Be(OH)(H_2O)_3^{+}$–$Be(H_2O)_4^{2+}$ aggregate by ~0.7 Å (Table 3). One $H_3O_2^{-}$ bridge then breaks and the beryllium center in one $Be(OH)(H_2O)_3^{+}$ is attacked by

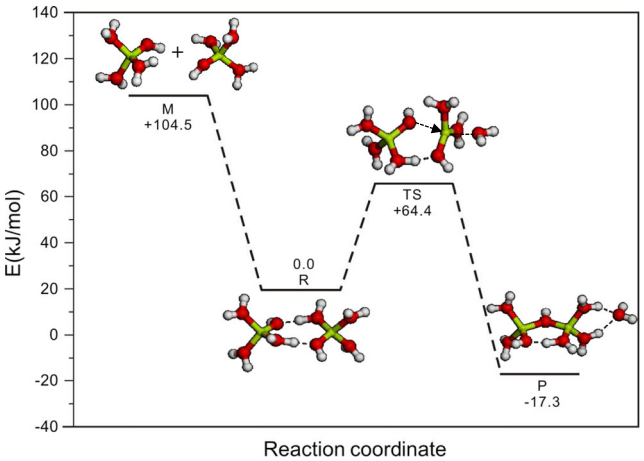

Fig. 2 Energy profile of the formation of $Be_2(OH)_2(H_2O)_5^{2+}$

Table 3 Bond lengths (Å) and bond angles (°) during the formation of $Be_2(OH)_2(H_2O)_5^{2+}$

	$Be(OH)(H_2O)_3^+$			$Be(OH)(H_2O)_3^+$		Be–Be	∠Be–OH–Be
	Be–OH	$Be–OH_2$	$Be–OH_2(L)$[a]	Be–OH	$Be–OH_2$		
R	3.564[b]	1.614	1.714	1.544	1.715	4.221	
	1.543[c]	1.722			1.721		
					1.613		
TS	2.320[b]	1.644	2.227	1.549	1.716	3.422	
	1.514[c]	1.667			1.726		
					1.612		
P	1.616[c]	1.692	4.741	1.624	1.719	2.913	128.1°
		1.688		1.538	1.728		
		1.593					

[a] Distance between the leaving water molecule and the attacked beryllium center

[b] Distance between the nucleophilic hydroxyl and the attacked beryllium center

[c] Distance between the attacked beryllium and its coordinated hydroxyl

the bound hydroxyl in the other $Be(OH)(H_2O)_3^+$. For the attacked $Be(OH)(H_2O)_3^+$, two bound waters and one hydroxyl constitute the equatorial plane of the trigonal bipyramidal transition state, and the remaining water molecule gradually leaves the beryllium center. After the transition state, the nucleophilic hydroxyl continues to approach the central beryllium and is eventually converted into a hydroxyl bridge connecting two beryllium atoms, which corresponds to the product (P). Meanwhile, the leaving water molecule enters the second coordination sphere of the dimeric product with a Be–OH_2 distance of 4.741 Å.

In contrast to the situation during the formation of $Be_2(OH)(H_2O)_6^{3+}$, there is always one $H_3O_2^-$ bridge present during the polymerization process, which leads to the shorter Be–Be distances in the transition state and product. Although deprotonation increases the tendency to aggregate, the activation barrier increases by ~15 kJ mol^{-1} relative to the formation of $Be_2(OH)(H_2O)_6^{3+}$. The reduced charge on the beryllium center caused by the addition of an hydroxyl group is considered to be responsible for this behavior (Table 6), which makes nucleophilic attack more difficult. In terms of the reaction energy, the reaction becomes less exothermic with deprotonation. If the reaction energy is based on nonaggregated monomeric beryllium (M), the reaction is more exothermic due to the high aggregation energy. Therefore, deprotonation promotes the polymerization of aqueous beryllium from a thermodynamic point of view, whereas deprotonation slows the rate of polymerization from a dynamic point of view. A planar pentameric ring composed of one hydroxyl bridge and one $H_3O_2^-$ bridge appears in the dimeric product, where the two Be–OH bonds of the bridging structure are both longer than those of the terminal hydroxyl group, suggesting that the bridging hydroxyl is labile. In addition, the angle ∠Be–OH–Be of 128.1° is much smaller than that in the $Be_2(OH)(H_2O)_6^{3+}$ dimer due to the presence of the $H_3O_2^-$ bridge. Interestingly, although the Be–OH_2(L) distance (between beryllium and the leaving water in the reactant) is much longer than that in the reactant during the formation of $Be_2(OH)(H_2O)_6^{3+}$, the activation energy barrier is higher. This indicates that the activation process is controlled by the nucleophilic attack, independent of the reactivity of the leaving bound water, which disagrees with the results of previous studies on aqueous aluminum species [34, 35].

Influence of X^- (X^- = F^-, Cl^-, Br^-) on the dimerization process

Since the bound water in aquo beryllium clusters can be substituted by a halide ion X^- (X^-= F^-, Cl^-, Br^-) [8], the influence of X^- on the chemical behavior of beryllium species deserves much attention. The dimerization process when one

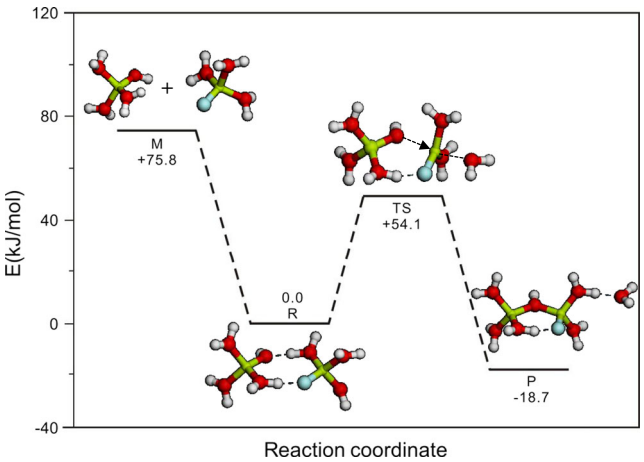

Fig. 3 Energy profile for the dimerization of $Be_2(OH)F(H_2O)_5^{2+}$

Table 4 Bond lengths (Å) and bond angles (°) during the formation of $Be_2(OH)F(H_2O)_5^{2+}$

	$BeF(H_2O)_3^+$				$Be(OH)(H_2O)_3^+$		Be–Be	∠Be–OH–Be
	Be–OH[a]	$Be–OH_2$	Be–F	$Be–OH_2(L)$[b]	Be–OH	$Be–OH_2$		
R	3.542	1.620	1.492	1.693	1.539	1.710	4.274	
		1.698				1.637		
						1.710		
TS	2.205	1.651	1.480	2.076	1.545	1.719	3.358	
		1.679				1.638		
						1.707		
P	1.659	1.647	1.504	3.700	1.584	1.704	2.899	126.7°
		1.709				1.622		
						1.691		

[a] Distance between the nucleophilic hydroxyl and the attacked beryllium center

[b] Distance between the leaving water molecule and the attacked beryllium center

of the aquo beryllium clusters contains an F^- rather than an OH^- ion is depicted in Fig. 3, and the corresponding structural parameters are listed in Table 4. One can see that the dimerization process is similar to that leading to the formation of $Be_2(OH)_2(H_2O)_5^{2+}$ as both products have the same charge; the only difference between them is that an $H_3O_2^-$ bridge in $Be_2(OH)_2(H_2O)_5^{2+}$ is replaced with an F–H_2O bridge during polymerization to the $Be_2(OH)F(H_2O)_5^{2+}$ dimer. For the formation of the latter dimer, the aggregation energy of 75.8 kJ mol^{-1} is in-between those of the $Be_2(OH)(H_2O)_6^{3+}$ and $Be_2(OH)_2(H_2O)_5^{2+}$ dimers (Table 5). The reduction in charge caused by the presence of F^- is responsible for the increased aggregation energy relative to that found for the formation of $Be_2(OH)(H_2O)_6^{3+}$, whereas the decreased aggregation energy relative to that found for the formation of $Be_2(OH)_2(H_2O)_5^{2+}$ is thought to be induced by the asymmetric bridging structure ($H_3O_2^-$ bridge and F–H_2O bridge) in the aggregate. It is observed that symmetric structures with strong hydrogen bonds are favored over asymmetric geometries, as pointed out in an earlier study [36]. Compared with the formation of $Be_2(OH)_2(H_2O)_5^{2+}$, a lower reaction energy (based on the M species) is observed due to their different aggregation energies. In contrast to the influence of deprotonation, the activation energy barriers do not change significantly when bound water is substituted by F^-. On the one hand, the higher electronegativity of fluorine than oxygen causes the charge on the beryllium in the Be–F bond to be more positive than in the Be–OH bond (Table 6), thereby making nucleophilic attack easier; on the other hand, replacing an H_2O with an anion such as OH^- decreases the charge on the attacked beryllium center (Table 6). Ultimately, these two opposing effects mean that the charge on the target beryllium is almost unchanged, as shown in Table 6. Therefore, the energy barriers of the present nucleophilic attack are barely influenced by the presence of F^-. In addition, the angle ∠Be–OH–Be in the $Be_2(OH)F(H_2O)_5^{2+}$ dimer is much less than that in $Be_2(OH)(H_2O)_6^{3+}$, and is closer to that in $Be_2(OH)_2(H_2O)_5^{2+}$ due to the presence of the F–H_2O bridge.

In order to elucidate the influences of other halide ions on dimerization, the dimerization process of the beryllium species containing a Cl^- or Br^- was simulated. The results show that the structures of every phase are similar to those found for the formation of $Be_2(OH)F(H_2O)_5^{2+}$, and the aggregation energies are also between those of $Be_2(OH)(H_2O)_6^{3+}$ and $Be_2(OH)_2(H_2O)_5^{2+}$ due to the asymmetric bridging structures. It can be seen from Table 6 that the Be–X distance increases in the order Be–F < Be–Cl < Be–Br. From Table 5, we can see that the activation barrier increases with reduced electronegativity, in agreement with the water-exchange behavior seen in Eldick's study [8]. This can largely be ascribed to the decrease in the positive charge on the attacked beryllium with decreasing electronegativity. The linear relationship between energy barrier and electronegativity (with a correlation coefficient of 0.992) is presented in Fig. 4, and it indicates that

Table 5 Energies relative to the reactant during the course of dimerization (values in kJ mol^{-1})

	$Be_2(OH)_2(H_2O)_5^{2+}$	$Be_2(OH)F(H_2O)_5^{2+}$	$Be_2(OH)Cl(H_2O)_5^{2+}$	$Be_2(OH)Br(H_2O)_5^{2+}$
M	104.5	75.8	67.2	65.1
R	0.0	0.0	0.0	0.0
TS	64.4	54.1	67.6	73.7
P	−17.3	−18.7	−22.8	−26.0

Table 6 Charges on the attacked beryllium and Be—L bond lengths ($L=OH^-$, X^-) in the reactant

Be species	q_{Be} (e)	Be–L (Å)
$Be_2(OH)(H_2O)_6^{3+}$	1.138	–
$Be_2(OH)_2(H_2O)_5^{2+}$	1.112	1.543
$Be_2(OH)F(H_2O)_5^{2+}$	1.136	1.492
$Be_2(OH)Cl(H_2O)_5^{2+}$	0.917	1.953
$Be_2(OH)Br(H_2O)_5^{2+}$	0.888	2.124

electronegativity is the key influence on the energy barriers for substituted ions with the same charge.

According to a previous study on the dimerization of other octahedral aqueous metal ions (such as $Al(H_2O)_6^{3+}$), in the first step a bound water molecule leaves the first coordination sphere to form the five-coordinate intermediate, which is then followed by nucleophilic attack [37]. In other words, the two steps are not concerted. For the tetrahedral beryllium species, the nucleophilic attack and the departure of bound water are concerted due to the lack of an intermediate. In view of their different dimerization mechanisms, the influences of an anion ligand on both octahedral and tetrahedral complexes should be considered. It is well documented that replacing a bound water molecule with OH^- and F^- enormously increases the lability of the remaining bound water for the octahedral aluminum species [38–41]. Undoubtedly, this substitution influences the first step in the dimerization of the aluminum species by promoting the departure of a bound H_2O. Although the influence of the anion on the second step is far from clear, it is possible that the influence of anions on the dimerization of aqueous aluminum is similar to the influence on the dimerization of aqueous beryllium, considering that the step and the formation process of beryllium dimer possess a similar nucleophilic attack behavior. If this is the case, this nucleophilic attack would become the rate-determining step in the dimerization of octahedral aluminum species, which requires further study. In addition, the formation of double hydroxyl bridges in the aluminum dimer differs from the formation of a single hydroxyl bridge in the beryllium dimer, and the influence of the anion on the formation of the second hydroxyl bridge should also be considered.

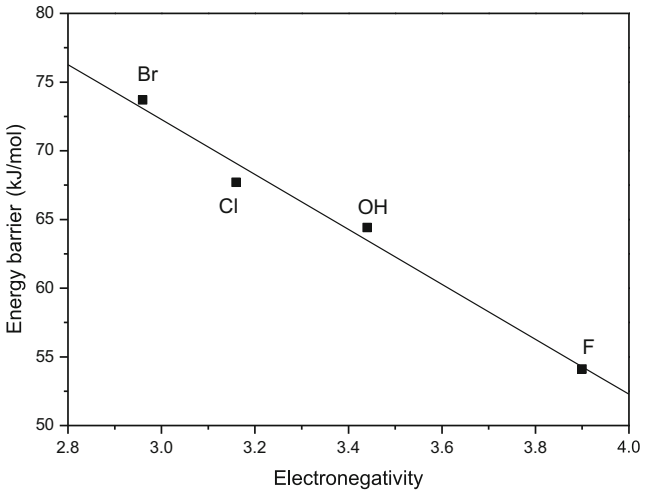

Fig. 4 Correlation of the activation energy barrier with the Pauling electronegativity of the substituted ligand

Conclusions

The dimerization of aqueous beryllium species was simulated in this study, changes in structure and energy were explored at the molecular scale, and the factors influencing polymerization were revealed. The results show that the polymerization is in essence a nucleophilic attack reaction, where one monomeric beryllium center is attacked by the bound hydroxyl of another monomeric beryllium complex. We can conclude that hydrolysis is a prerequisite for polymerization, as it provides the hydroxyl group that acts as the nucleophilic reagent. The charge and electronegativity of the ligands that are added to monomeric beryllium via the substitution of bound water molecules are key to influencing dimerization. Adding an anionic ligand leads to a decrease in the charge on the central beryllium, thereby increasing the energy of the barrier to nucleophilic attack. In contrast, high anion electronegativity increases the positive charge on beryllium, thereby decreasing the barrier height. Therefore, there is no doubt that both of these factors should be considered in detail when attempting to enhance or restrain dimerization in practice. In addition, the aggregation energy is influenced by the imported negative charge and the symmetry of the bridging structure in the aggregate, so it exhibits different behavior from that of the energy barrier.

Acknowledgments This project was supported by the National Natural Science Foundation of China (no. 21303021) and the Natural Science Foundation of Anhui Province (no. 1408085QB39), as well as the Foundation for Young Talents in College of Anhui Province under grant no. 2012SQRL117. Further support from the Anhui Provincical Key Laboratory for Degradation and Monitoring of Pollution of the Environment is acknowledged.

References

1. Schmidbaur H (2001) Recent contributions to the aqueous coordination chemistry of beryllium. Coord Chem Rev 215(1):223–242
2. Rossman MD, Preuss OP, Powers MB (1991) Beryllium: biomedical and environmental aspects. Williams and Wilkins, Baltimore
3. Karus F, Baer SA, Buchner MR, Karttunen AJ (2012) Reactions of beryllium halides in liquid ammonia: the tetraammineberyllium cation $[Be(NH_3)_4]^{2+}$, its hydrolysis products, and the action of Be^{2+} as a fluoride-ion acceptor. Chem Eur J 18(7):2131–2142

4. Alderighi L, Gans P, Midollini S, Vacca A (2000) Aqueous solution chemistry of beryllium. Adv Inorg Chem 50:109–172
5. Scott BL, McCleskey TM, Chaudhary A, Hong-Geller E, Gnanakaran S (2008) The bioinorganic chemistry and associated immunology of chronic beryllium disease. Chem Commun 25: 2837–2847
6. Dehnicke K, Neumüller B (2008) News from the chemistry of berylliums. Z Anorg Allg Chem 634(15):2703–2728
7. Wong CY, Woolins JD (1994) Beryllium coordination chemistry. Coord Chem Rev 130(1–2):243–273
8. Budimir A, Walther M, Puchta R, van Eldik R (2011) Ligand exchange processes on solvated beryllium cations. V. Water exchange on $[BeX(H_2O)_3]^+$ (X= H^-, F^-, Cl^-, Br^-, OH^-, CN^-, $NCNCN^-$). Z Anorg Allg Chem 637(5):515–522
9. Cecconi F, Ghilardi CA, Midollini S, Orlandini A, Mederos A (1998) Isolation of $[Be_3(\mu\text{-}OH)_3(H_2O)_6]^{3+}$. Synthesis, ^9Be NMR spectroscopy, and crystal structure of $[Be_3(\mu\text{-}OH)_3(H_2O)_6](picrate)_3\cdot 6H_2O$. Inorg Chem 37(1):146–148
10. Massa W, Dehnicke K (2007) $[Be(OH_2)_4]Cl_2$—product, IR spectrum and crystal structure. Z Anorg Allg Chem 633(9):1366–1370
11. Dance IG, Freeman HC (1969) Refinement of the crystal structure of beryllium sulphate tetrahydrate. Acta Crystallogr B 25:304–310
12. Wildner M, Stoilova D, Georgiev M, Karadjova V (2004) Beryllium selenate tetrahydrate, $BeSeO_4\cdot 4H_2O$: crystal structure and infrared spectroscopy. J Mol Struct 707(1–3):123–130
13. Schmidt M, Schier A, Rieed J, Schmidbaur H (1998) The novel binuclear hydroxyberyllate species $[Be_2(OH)_7]^{3-}$ and the hydroxide hydrate anion $[H_3O_2]^-$ as components of beryllate equilibria. Inorg Chem 37(14):3452–3453
14. Schmidbaur H, Schmidt M, Schier A, Riede J, Tamm T, Pyykkö P (1998) Identification and structural characterization of the predominant species present in alkaline hydroxyberyllate solutions. J Am Chem Soc 120(12):2967–2968
15. Plieger PG, John KD, Keizer TS, McCleskey TM, Burrell AK, Martin RL (2004) Predicting ^9Be nuclear magnetic resonance chemical shielding tensors utilizing density functional theory. J Am Chem Soc 126(44):14651–14658
16. Puchta R, van Eikema Hommes N, van Eldik R (2005) Evidence for interchange ligand-exchange processes on solvated beryllium cations. Helv Chim Acta 88(5):911–922
17. Asthagiri D, Pratt LR (2003) Quasi-chemical study of Be^{2+}(aq) speciation. Chem Phys Lett 371(5–6):613–619
18. Tossell JA (1998) The effect of hydrolysis and oligomerization upon the NMR shieldings of Be^{2+} and Al^{3+} species in aqueous solution. J Magn Reson 135(1):203–207
19. Wander MCF, Rustad JR, Casey WH (2010) Influence of explicit hydration waters in calculating the hydrolysis constants for geochemically relevant metals. J Phys Chem A 114(4):1917–1925
20. Frisch MJ, Trucks GW, Schlegel HB, Scuseria GE, Robb MA, Cheeseman JR, Montgomery JA, Vreven T, Kudin KN, Burant JC, Millam JM, Iyengar SS, Tomasi J, Barone V, Mennucci B, Cossi M, Scalmani G, Rega N, Petersson GA, Nakatsuji H, Hada M, Ehara M, Toyota K, Fukuda R, Hasegawa J, Ishida M, Nakajima T, Honda Y, Kitao O, Nakai H, Klene M, Li X, Knox JE, Hratchian HP, Cross JB, Bakken V, Adamo C, Jaramillo J, Gomperts R, Stratmann RE, Yazyev O, Austin AJ, Cammi R, Pomelli C, Ochterski JW, Ayala PY, Morokuma K, Voth GA, Salvador P, Dannenberg JJ, Zakrzewski VG, Dapprich S, Daniels AD, Strain MC, Farkas O, Malick DK, Rabuck AD, Raghavachari K, Foresman JB, Ortiz JV, Cui Q, Baboul AG, Clifford S, Cioslowski J, Stefanov BB, Liu G, Liashenko A, Piskorz P, Komaromi I, Martin RL, Fox DJ, Keith T, Al-Laham MA, Peng CY, Nanayakkara A, Challacombe M, Gill PMW, Johnson B, Chen W, Wong MW, Gonzalez C, Pople JA (2004) Gaussian 03 (revision B.02). Gaussian, Inc., Wallingford
21. Becke AD (1993) Density-functional thermochemistry: III. The role of exact exchange. J Chem Phys 98(7):5648–5652
22. Lee C, Yang W, Parr RG (1988) Development of the Colle-Salvetti correlation-energy formula into a functional of the electron density. Phys Rev B 37(2):785–789
23. Stevens PJ, Devlin FJ, Chablowski CF, Frisch MJ (1994) Ab initio calculation of vibrational absorption and circular dichroism spectra using density functional force fields. J Phys Chem 98(45):11623–11627
24. Gonzalez C, Schlegel HB (1989) An improved algorithm for reaction path following. J Chem Phys 90(4):2154–2161
25. Gonzalez C, Schlegel HB (1990) Reaction path following in mass-weighted internal coordinates. J Phys Chem 94(14):5523–5527
26. Miertus S, Scrocco E, Tomasi J (1981) Electrostatic interaction of a solute with a continuum. A direct utilizaion of *ab initio* molecular potentials for the prevision of solvent effects. Chem Phys 55(1):117–129
27. Miertus S, Tomasi J (1982) Approximate evaluations of the electrostatic free energy and internal energy changes in solution processes. Chem Phys 65(2):239–245
28. Hofmann H, Hansele E, Clark T (1990) A cautionary note on the use of the frozen-core approximation for correlation energy calculations involving alkali metals. J Comput Chem 11(10):1147–1150
29. Puchta R, van Eldik R (2008) Ligand-exchange processes on solvated beryllium cations. Which model reaction is preferable for quantum-chemical investigations of a water-exchange mechanism? Helv Chim Acta 91(6):1063–1071
30. Puchta R, Pasgreta E, van Eldik R (2009) Ligand exchange processes on the smallest solvated alkali and alkaline earth metal cations: an experimental and theoretical approach. Adv Inorg Chem 61:523–571
31. Ardon M, Bino A (1985) Role of the H_3O_2 bridging ligand in coordination chemistry. 1. Structure of hydroxoaquametal ions. Inorg Chem 24(9):1343–1347
32. Bino A, Gibson DJ (1982) The hydrogen oxide bridging ligand ($H_3O_2^-$). 1. Dimerization and polymerization of hydrolyzed trinuclear metal cluster ions. J Am Chem Soc 104(16):4383–4388
33. Ardon M, Bino A (1987) A new aspect of hydrolysis of metal ions: the hydrogen-oxide bridging ligand ($H_3O_2^-$). Struct Bond 65:1–28
34. Loring JS, Casey WH (2002) A correlation for establishing solvolysis rates of aqueous Al(III) complexes: a possible strategy for colloids and nanoparticles. J Colloid Interface Sci 251(1):1–9
35. Jin XY, Qian ZS, Lu BM, Yang WJ, Bi SP (2011) Density functional theory study on aqueous aluminum-fluoride complexes: exploration of the intrinsic relationship between water-exchange rate constants and structural parameters for monomer aluminum complexes. Environ Sci Technol 45(1):288–293
36. Perrin CL, Thoburn JD (1992) Symmetries of hydrogen bonds in monoanions of dicarboxylic acids. J Am Chem Soc 114(22):8559–8565
37. Qian ZS, Feng H, Zhang ZJ, Yang WJ, Jin J, Miao Q, He LN, Bi SP (2009) Theoretical investigation on the dimerization of the deprontonated aqua ion of Al(III) in water. Dalton Trans 3:521–529
38. Phillips BL, Casey WH, Crawford SN (1997) Solvent exchange in $AlF_x(H_2O)_{6-x}^{3-x}$ (aq) complexes: ligand-directed labilization of water as an analogue for ligand-induced dissolution of oxide minerals. Geochim Cosmochim Acta 61(15):3041–3049
39. Yu P, Phillips BL, Casey WH (2001) Water exchange in fluoroaluminate complexes in aqueous solution: a variable temperature multinuclear NMR study. Inorg Chem 40(18): 4750–4754
40. Nordin JP, Sullivan DJ, Phillips BL, Casey WH (1998) An ^{17}O NMR study of the exchange of water on $AlOH(H_2O)_5^{2+}$(aq). Inorg Chem 37(19):4760–4763
41. Phillips BL, Tossell JA, Casey WH (1998) Experimental and theoretical treatment of elementary ligand exchange reactions in aluminum complexes. Environ Sci Technol 32(19):2865–2870